Supratidal Land Use Change and Its Morphodynamic Effects along the Eastern Coast of Laizhou Bay during the Recent 50 Years

Authors: Wang, Qing, Zhong, Shaoyun, Li, Xueyan, Zhan, Chao, Wang, Xin, et al.

Source: Journal of Coastal Research, 74(sp1) : 83-94

Published By: Coastal Education and Research Foundation

URL: https://doi.org/10.2112/SI74-008.1

Journal of Coastal Research	SI	74	83–94	Coconut Creek, Florida	2016

Supratidal Land Use Change and Its Morphodynamic Effects along the Eastern Coast of Laizhou Bay during the Recent 50 Years

Qing Wang[‡*], **Shaoyun Zhong**[‡], **Xueyan Li**[‡], **Chao Zhan**[‡], **Xin Wang**[‡], **and Peng Liu**[‡]

[‡] Coast Institute, Ludong University
Yantai, Shandong 264025, P. R. China
schingwang@126.com

www.cerf-jcr.org

www.JCRonline.org

ABSTRACT

Wang, Q.; Zhong, S.Y.; Li, X.Y.; Zhan, C.; Wang X., and Liu, P., 2016. Supratidal land use change and its morphodynamic effects along the eastern coast of Laizhou Bay during the recent 50 years. *In*: Harff, J. and Zhang, H. (eds.), *Environmental Processes and the Natural and Anthropogenic Forcing in the Bohai Sea, Eastern Asia. Journal of Coastal Research*, Special Issue, No. 74, pp. 83–94. Coconut Creek (Florida), ISSN 0749-0208.

Using nautical charts, topographic maps, high resolution remote sensing images and field observation, this study analyzed the land use change of the supratidal zone and its coastal morphodynamic effects along the eastern coast of Laizhou Bay. The results show that land use along the eastern coast of Laizhou bay has been significantly changed in the recent 50 years. The main evolution trend is the transition from aeolian sandy land, woodland and farmland to aquaculture ponds and residential land since the early 1990s. A belt zone of aquaculture facility parallel to the coastline has been formed and dykes are constructed along the outside of the coastal aquiculture zone. The significant land cover change in the supratidal zone has profoundly modified the boundary conditions of storm surges. The hydrodynamic modeling results show that the ocean dynamics near the coastline are enhanced and caused severe erosion of the coastline, beach and underwater coastal sea slope along the eastern coast of Laizhou Bay over the recent 30 years.

ADDITIONAL INDEX WORDS: *Eastern coast of Laizhou Bay, supratidal zone, land use change, temperate monsoon sandy coast, factory aquaculture facility, ocean dynamics.*

INTRODUCTION

More than 60% of the global population lives in the coastal zone and it is anticipated to reach 75% in decades (Airoldi and Beck, 2007). The length of sandy coast accounts for more than 50% of the global coastal length (Short and Masselink, 1999). About 60 ~ 70% of the global sandy coasts has been eroded (Bird, 1996; Durgappa, 2008) due to enhanced ocean dynamics caused by global change (Komar and Allan, 2008; Mather, 2008), the sediment dynamic change (Splinter *et al.*, 2012; Zhang, Douglas and Leatherman, 2004) and human activities (Defeo *et al.*, 2009). In China, sandy coast accounts for about 22% of the total coastal length, 70% of the sandy coast is eroded (Xia, 2009). Coastal erosion onshore and sediment accretion offshore change coastal geomorphology at time scales of decades to centuries, causing overall recession of the coastline and serious social consequences. Large amount of research have been devoted to study anthropogenic forces of coastal erosion including decrease of sediment discharge, sand mining, and coastal engineering structures. However, few researches have been conducted to investigate coastal morphology change caused by land use change in the supratidal zone.

Serious erosion in the eastern coast of Laizhou Bay has been observed since the 1960s (Zhuang, Chen and Xu, 1989) and has been studied since mid-1980s. Decrease of sediment discharge caused by construction of reservoirs in the northwestern mountain of Jiaodong Peninsula from the late 1950s to the early 1960s was considered as the main cause of coastal erosion (Chang, Zhuang and Wu, 1993; Wang *et al.*, 2003; Zhuang, Chen and Xu, 1989). It was expected that a new equilibrium state of coastal erosion/accretion would be reached as the reservoir's impact on the fluvial sediment transport gradually wear off and the rate of coastal erosion will be reduced. However, our field surveys show that the coast is still far from equilibrium state 50 years after the construction of the reservoirs. In the last 30 years, the extent and scale of coastal erosion continued to broaden. Erosive scarps has been formed and beaches became narrower and steeper. It is speculated that aquaculture facilities built in the aeolian sandy land of the supratidal zone in the last 30 years might be a cause of the coastal erosion. Therefore, this study focuses on revealing the spatio-temporal change of the supratidal land cover and its impact on coastal erosion.

Study region

The sandy coast on the southeast of Bohai Sea and northwest of Jiaodong Peninsula is developed along the narrow piedmont depo-

DOI: 10.2112/SI74-008.1 received (12 Febuary 2015); accepted in revision (25 January 2016).

sitional plain. The east section (from Luanjiakou to Qimu Island) is a straight sandy coast from NE to WS. The west section (from Diaolongzui spit to Hutouya) is an arc-shaped coast from NW to ES. The middle section (from Qimu Island to Diaolongzui spit) is a compound headland-bay coast from NE to WS (Figure 1). Part of the middle section, from Jiehe mouth to Diaolongzui spit is investigated in great detail in this study.

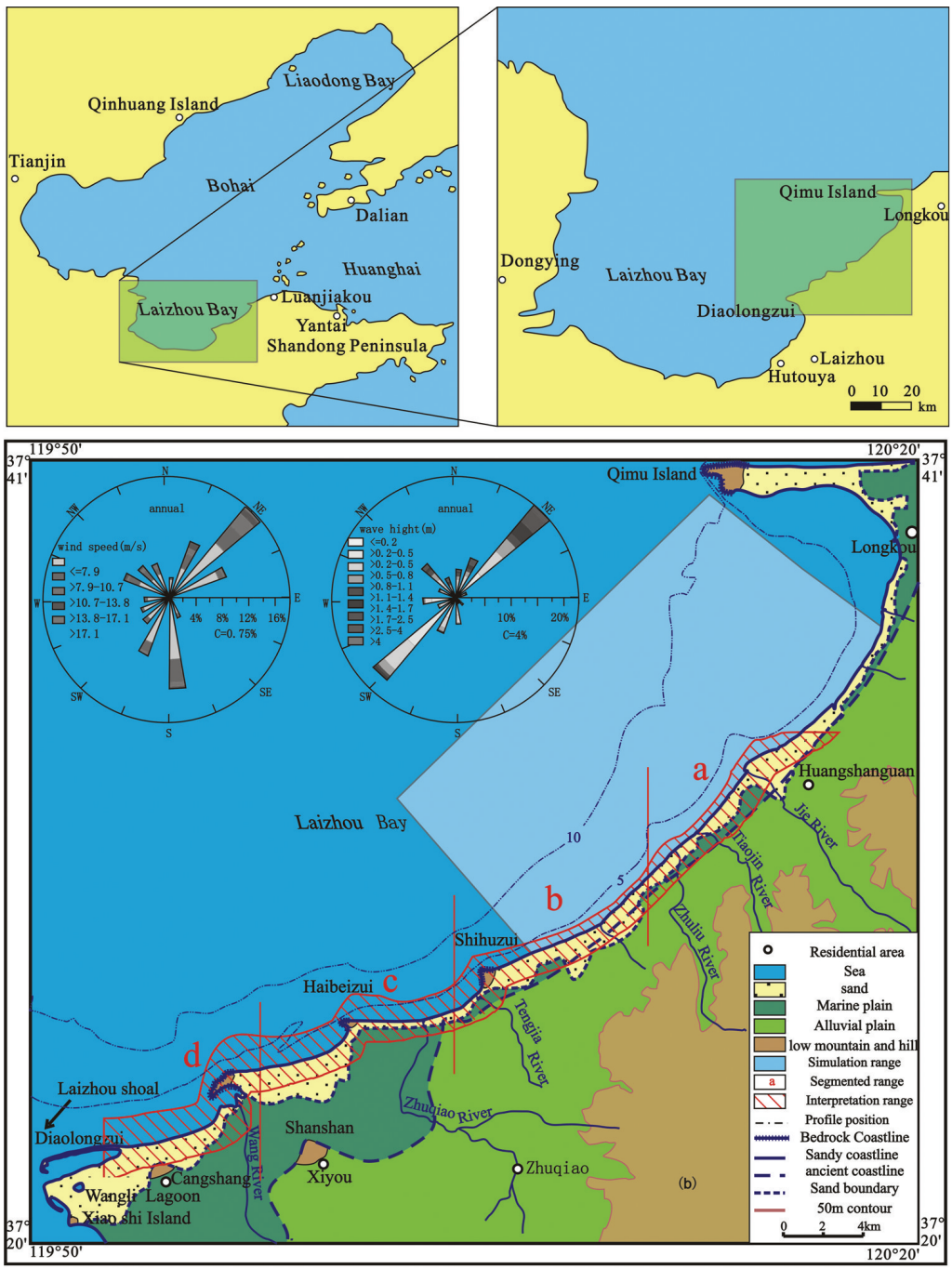

Figure 1. Location map of the study region. The map is drawn based on the chart of 1∶100 000 scale from Weihe mouth to Longkou harbor in 1959. The coast is divided into the four sections of a, b, c and d to show clearly the land use change of the intertidal zone

The region is controlled by temperate continental monsoon climate. The wind direction in summer and that in winter are mainly S-SE and NNE-N-NW, respectively. The directions of the strongest wind and the dominated wind are both NE, and that of the secondary dominated wind is S. The directions of the dominated wave is NE and the secondary dominated wave is WS, both parallel to the coastline (Edition Committee of the Bay Chorography in China, 1993; Zhuang, Chen and Xu, 1989). The mean tidal range is only about 1.0 m. The region is susceptible to storm surges under the control of extratropical cyclones. From 1951 to 2013, a total of 21 severe storm surges took place in Laizhou Bay. During storm surges, the maximum sea level can reach up to 6.74 m (Table 1). Through long-term interaction of longshore sediment flow, storm surges and wind, the east of Laizhou Bay developed a sandy coast consisting of subaqueous sandy dykes, intertidal beach, broad supratidal zone, landside sandy dunes, and aeolian sandy land. The average width of intertidal zone is 250 ~ 450 m, and the maximum width reaches up to 1000 m.

METHODS

The 2km-width strip zone parallel to the coastline is chosen as the region of the interpretation. The geographic data include: 1∶50 000 topographic map measured in 1969; 1∶10 000 topographic maps measured from 1984 to 1985; remote sensing image from SPOT satellite on October 20, 1998, ALOS satellite on October 16, 2006 and ZY-3 satellite on April 7, 2013. Detailed information such as measurement/imaging time, quantity, scale or resolution of data source are listed in Table 2.

The topographic maps are digitized and processed with the method of visual interpretation. The satellite remote sensing images are preprocessed by registration, fusion and the mask technology. Land use interpretation of the supratidal zone are based on land use classification (GB/T 21010-2007) and divided into 8 types: sandy land, woodland, garden, farmland, residential land, river, aquaculture land and sea (Table 3). The results are verified and corrected by field investigation. Coastline, isobaths and water depth data are extracted from nautical chart of 1985 (scale of 1∶250 000) and elevation data were digitized from topographic map of 1983 (scale of 1∶10 000).

With the support of Mike21 published by DHI, a tidal current field model is established through the numerical integration of horizontal momentum equation and continuity equation based on the two-dimensional shallow water equations. The two horizontal momentum equations for the x- and y-component, and the local continuity equation are expressed by:

$$\frac{\partial h\bar{u}}{\partial t}+\frac{\partial h\bar{u}^2}{\partial x}+\frac{\partial h\bar{v}\bar{u}}{\partial y}=f\bar{v}h-gh\frac{\partial \eta}{\partial x}-\frac{h}{\rho_0}\frac{\partial p_a}{\partial x}-\frac{gh^2}{2\rho_0}\frac{\partial \rho}{\partial x}+\frac{\tau_{sx}}{\rho_0}-\frac{\tau_{bx}}{\rho_0}-\frac{1}{\rho_0}\left(\frac{\partial s_{xx}}{\partial x}+\frac{\partial s_{xy}}{\partial y}\right)+\frac{\partial}{\partial x}(hT_{xx})+\frac{\partial}{\partial y}(hT_{xy})+hu_s s \quad (1)$$

$$\frac{\partial h\bar{v}}{\partial t}+\frac{\partial h\bar{u}\bar{v}}{\partial x}+\frac{\partial h\bar{u}^2}{\partial y}=-f\bar{u}h-gh\frac{\partial \eta}{\partial y}-\frac{h}{\rho_0}\frac{\partial p_a}{\partial y}-\frac{gh^2}{2\rho_0}\frac{\partial \rho}{\partial y}+\frac{\tau_{sy}}{\rho_0}-\frac{\tau_{by}}{\rho_0}-\frac{1}{\rho_0}\left(\frac{\partial s_{yx}}{\partial x}+\frac{\partial s_{yy}}{\partial y}\right)+\frac{\partial}{\partial x}(hT_{xy})+\frac{\partial}{\partial y}(hT_{yy})+hv_s s \quad (2)$$

$$\frac{\partial h}{\partial t}+\frac{\partial h\bar{u}}{\partial x}+\frac{\partial h\bar{v}}{\partial y}=hs \quad (3)$$

Table 1. *Statistics of severe storm surges along the eastern Laizhou Bay in the last* 60 *years*

Occurrence time	Storm surge type	Maximum tidal level (m)	Mean wind force (class)	Action time (hours)	Direction of wind, wave (the eastern coast)
1952-12-20	Extratropical	6.15	11	48	NE/NW
1960-04-10	Extratropical	5.95	10	48	NE/NW
1964-04-06	Extratropical	6.24	10	48	NE/NW
1967-11-19	Extratropical	5.50	10	48	NE/NW
1969-04-23	Extratropical	6.74	10	48	NE/NW
1973-07-26	Typhoon-induced	4.10	9	36	NE/NW
1977-05-13	Extratropical	5.00	9	36	NE/NW
1980-04-05	Extratropical	6.01	8	48	NE/NW
1985-08-19	Typhoon-induced	5.30	9	36	NE/NW
1987-10-29	Extratropical	4.00	9	48	NE/NW
1987-11-26	Extratropical	5.83	10	48	NE/NW
1992-08-31	Typhoon-induced	6.45	10	60	NE/NW
1997-08-19	Typhoon-induced	5.90	8	48	NE/NW
2000-04-09	Extratropical	4.10	8	24	NE/NW
2003-10-11	Extratropical	6.24	8	48	NE/NW
2007-03-04	Extratropical	5.70	8	36	NE/NW
2009-04-15	Extratropical	3.50	8	48	NE/NW
2010-10-25	Extratropical	/	8	48	NE/NW
2011-09-01	Extratropical	3.11	8	48	NE/NW
2012-07-31	Typhoon-induced	/	9	36	NE/NW
2013-05-26	Extratropical	/	9	72	NE/NW

Table 2. *Topographic maps and remote sensing images of the eastern coast of Laizhou Bay in the different periods*

Data sources	Measurement/Imaging time	Resolution	Map
Topographic maps	1969	1 :50 000	5
Topographic maps	1985	1 :10 000	18
SPOT sensing images	1998	multiband 20 m	3
SPOT sensing images	1998	Panchromatic 10 m	1
ALOS sensing images	2006	multiband 10 m	3
ALOS sensing images	2006	Panchromatic 2.5 m	1
ZY-3 sensing images	2013	multiband 5.8 m	3
ZY-3 sensing images	2013	Panchromatic 2.1 m	1

Table 3. *Land use types and their interpretation signs of remote sensing images in the eastern coastal zone of Laizhou Bay*

Type	Implication	Interpretation signs		
		Shape	Tone	Texture
Sea	Including beach and parts of water	Contiguous sheet	Blue or dark blue	Uniform
River	Riverway including washland and riverbed	Irregular strip	blue	Uniform
Woodland	Shelter forest	Sheet or strip	Dark red	Relatively uniform
Garden	Dominated by apple orchard	Block	Red	Unobvious
Farmland	Including dry land and vegetable field	Block with clear boundary	Bright red	Fine and smooth
Residential land	Residential land	Sheet with obvious geometrical feature	Gray	Coarse
Aquaculture land	Aquaculture ponds and greenhouse	Block with clear boundary	Dark blue	Relatively uniform
Sandy land	Landside aeolian sandy land excluding shelter forest	strip	White or light white	Obvious

where t is the time; x and y are the Cartesian co-ordinates; $h=\eta+d$ is the total water depth; d is the still water depth; η is the surface elevation; $\bar{u}$ and $\bar{v}$ are the velocity components in the x and y direction; $f=2\ \Omega\sin\phi$ is the Coriolis parameter (Ω is the angular rate of revolution and ϕ is the geographic latitude); g is the gravitational acceleration; ρ is the density of water; ν_t is the vertical turbulent (or eddy) viscosity; p_a is the atmospheric pressure; ρ_0 is the reference density of water; s is the magnitude of the discharge due to point sources; u_s and ν_s are the velocity components by which the water is discharged into the ambient water; s_{xx}, s_{xy}, s_{yx} and s_{yy} are components of the radiation stress tensor; T_{xx}, T_{xy}, T_{yx} and T_{yy} are components of viscous force; τ_{sx} and τ_{sy} are the x and y components of the surface wind; τ_{bx} and τ_{by} are the x and y components of the bottom stress.

A wave field model is built on the wave action conservation equation showed in the equation (4).

$$\frac{\partial A}{\partial t}+\nabla_x\cdot(c_gA)+\nabla_\theta\cdot(c_\theta A)+\nabla_\sigma\cdot(c_\sigma A)=S \quad (4)$$

where $\frac{\partial A}{\partial t}$ is wave energy varying with time; $\nabla_x\cdot(c_gA)$ is wave energy varying with geographic space; $\nabla_\theta\cdot(c_\theta A)$ is wave energy varying with direction; $\nabla_\sigma\cdot(c_\sigma A)$ is wave energy varying with frequency; S is source function.

Sediment transport model under the joint action of wave and tidal current is set up based on the convection diffusion equation taking into account the sediment deposition shown in the equation (5).

$$\frac{\partial\bar{C}}{\partial t}+u\frac{\partial\bar{C}}{\partial x}+v\frac{\partial\bar{C}}{\partial y}=\frac{1}{h}\frac{\partial}{\partial x}\left(hD_x\frac{\partial\bar{C}}{\partial x}\right)+\frac{1}{h}\frac{\partial}{\partial y}\left(hD_y\frac{\partial\bar{C}}{\partial y}\right)+\sum_{i=1}^{n}\frac{S_i}{h} \quad (5)$$

where u and v are the velocity components in the x and y direction; $\bar{C}$ is sediment concentration; D_x and D_y are diffusion coefficient components in the x and y direction; n is the total numbers of source and sink; i is the number of source and sink and the meanings of the other variables are the same as the above.

According to the tidal characteristics of Laizhou Bay, the numerical simulation range is from east LONG. 120.03 to 120.24 and north LAT. 37.35 to 37.62. One endpoint of the open boundary islocated in east LONG. 120.03 and north LAT. 37.52, the other is located in east LONG. 120.17 and north LAT. 37.62. The computational grids are generated with the help of SMS employing the finite volume method (Figure 2). The grid length is set as 25 m near the coastline and gradually increases to 700 m in the open sea to improve computational efficiency and accuracy. According to the topographic map of 1985 and the field survey, the width of the supratidal zone in the study region is set as 450 m, assuming the aquaculture facility zone extending from land to sea.

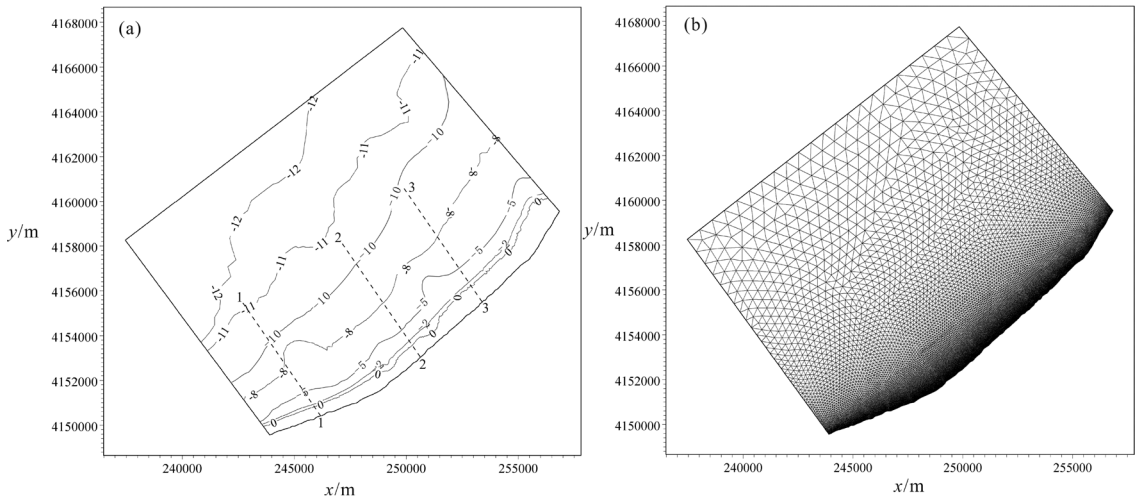

Figure 2. The water depths(a) and grids(b) for coastal morphodynamic effects of the narrowing supratidal zone in the study region. The results of wave height, current velocity and geomorphic effects are extracted along the profiles 1-1, 2-2 and 3-3

Figure 3. Land use change of the supratidal zone along the eastern coast of Laizhou Bay (a. a part of topographic map of 1∶10 000 scale in 1984; b. the same position of remote sensing image in 2013). The blue line represents coastline

The simulation time length and the time step interval are set as 24 hours and 600 s, respectively. For the open boundary, the water level is provided by tidal prediction of Mike21; the significant wave height is set as 4.5 m and wave direction is set as NE according to the data of "10.11" storm surge data along Laizhou Bay. The land boundary is set as a vertical wall and the location varies with the different land use extent. The wet-dry scheme is applied in the model in view of the waterline changing with the tidal level. The drying depth is set as 0.005 m; the flooding depth is set as 0.05 m; the wetting depth is set as 0.1 m. The coefficient *Cs* of Smagorinsky is set as 0.28; the manning number is 32; Coriolis force varies with latitude.

The median diameter(d_{50}) of sediments is from 0.063 mm to 0.2 mm on the basis of *The Bay Chorography in China*(3). The settling velocity is computed by Stokes Formula shown in the equation(6).

$$w_0 = \frac{g}{18\mu}\left(\frac{\rho_s - \rho_w}{\rho_w}\right) d_{50}^{\ 2} \qquad (6)$$

where w_0 is the settling velocity of a single sediment; μ is vis-

cosity coefficient; ρ_s is dry density of sediment; ρ_w is seawater density.

The critical incipient velocity is computed by Wushui Formula shown in the equation(7).

$$u_e = \left(\frac{h}{d_{50}}\right)^{0.14}\left(17.6\frac{\gamma_s-\gamma}{\gamma}d_{50} + 0.000000605\frac{10+h}{d_{50}^{0.72}}\right)^{0.5} \quad (7)$$

where u_e is the critical incipient velocity; γ_s and γ are the density of sediment and water respectively.

The critical settling velocity is computed by Feiyuqing Formula shown in the equation(8).

$$u_d = 0.812d_{50}^{0.4}(\omega_s h)^{0.2} \quad (8)$$

where u_d is the critical settling velocity; ω_s is the settling velocity of sediments(mm/s).

Based on the above premise, we calculate the coastal morphodynamic effects of the above-mentioned storm surge for 12 and 24 hours in three cases: (1) unused supratidalzone(*i. e.* 0% land use), (2) 150m-width aquaculture facility zone parallel to the coastline built along the supratidal zone(*i. e.* 30% land use), (3) 300m-width aquaculture facility zone parallel to the coastline built along the supratidal zone(*i. e.* 70% land use). At the same time, wave height, current velocity and geomorphic evolution along the three profiles 1-1, 2-2 and 3-3(Figure 2) extracted from the above results respectively are discussed in the following sections.

RESULTS

Land use change along the coastal zone

Land use in 1969 was dominated by woodland, farmland and sandy land, which occupied 30.99%, 22.08% and 16.26% of the total area, respectively(Table 4). It was still dominated by woodland, sandy land and farmland in 1985 but the area of farmland experienced a significant decline. In 1998, the area of sandy land reduced to 9.47% of the total area. More importantly, aquaculture land occupied 11.85% of the total area. The dominant land use was changed to woodland, farmland and aquaculture land. The area of residential land also started to increase. In 2013, the main land use type turned to woodland, aquaculture land, farmland and residential land, which occupied 23.37%, 19.45%, 12.86% and 12.25% of the total area respectively. Overall, the areas of residential land and aquaculture land began to increase rapidly after 1985, while sandy land and farmland decreased(Table 4).

The area of sandy land decreased sharply from 9.59 km^2 in 1985 to 5.71 km^2 in 1998, to 2.05 km^2 in 2006, to 1.88 km^2 in 2013. The area of residential land increased significantly, with the growth rate being 99.35%, 91.48% and 26.37% of each period respectively after 1985. Aquaculture land emerged in 1985 and occupied 7.14 km^2, 9.48 km^2 and 11.72 km^2, in 1998, 2006, and 2013, respectively (Table 5).

It is revealed from the transition matrixes of different land use types in different periods(Table 6, Table 7, Table 8 and Table 9) that there has been a general trend of shifting from sandy land, woodland and farmland to aquaculture land and residential land in the past 50 years. From 1969 to 1985, 2.72 km^2 of sandy land was turned into sea, showing coastal erosion from 1969 to 1985(Table 6).

From 1985 to 1998, the main evolution trend is the transition from sandy land and woodland to aquaculture land by a net area of 3.29 km^2 and 3.02 km^2, respectively. Sandy land was converted to sea by a net area of 1.57 km^2, and 1.74 km^2 of woodland was converted to sandy land(Table 7).

From 1998 to 2006, the main evolution trend is the transition from sandy land to aquaculture land by a net area of 2.97 km^2. The sea area decreased by a net 1.63km^2, showing that the coast changed from retreating landward to extending seaward. The majority (1.35 km^2) of the created land was occupied by the artificial facilities, such as residential land and aquaculture ponds(Table 8). Meanwhile, the decrease of sandy land area reached to 3.81 km^2 from 1985 to 1998(Table 7). From 2006 to 2013, the sea area decreased by the net 0.74 km^2 but the artificial facilities such as residential land and aquaculture ponds occupied 0.85 km^2 sea area. At the same time, the sandy land decreased by a net area of 0.21 km^2(Table 9).

Table 4. *Land use types and their areas along the eastern coast of Laizhou Bay in the different periods*

Time	Sea	Sandy land	Woodland	Garden	Farmland	Residential land	River	Aquaculture land	Total
1969	15.21	9.84	18.75	0.91	13.36	1.63	0.81	0	60.51
1985	18.10	9.59	20.24	2.97	7.37	1.53	0.71	0	60.51
1998	19.37	5.71	16.74	0	7.4	3.05	0.86	7.14	60.27
2006	17.57	2.05	14.65	0	10.07	5.84	0.63	9.48	60.29
2013	16.83	1.88	14.08	0	7.75	7.38	0.62	11.72	60.26

Table 5. *Change rates of different land use types along the eastern coast of Laizhou Bay from* 1969 *to* 2013 (%)

Time	Sea	Sandy land	Woodland	Garden	Farmland	Residential land	River	Aquaculture land
1969-1985	19.00	-2.54	7.95	226.37	-44.84	-6.13	-12.35	—
1985-1998	7.02	-40.46	-17.29	-100.00	0.41	99.35	21.13	—
1998-2006	-9.29	-64.10	-12.49	—	36.08	91.48	-26.74	32.77
2006-2013	-4.21	-8.29	-3.89	—	-23.04	26.37	-1.59	23.63

Notes: plus means the increase of area, minus means the decrease of area, horizontal line means the absence of the type

Table 6. *Transition matrix of different land use types along the eastern coast of Laizhou Bay from* 1969 *to* 1985(km^2)

1969–1985	Sea	Sandy land	Woodland	Garden	Farmland	Residential land	Aquaculture land	Total
Sea	15.20	0.06	0	0	0.03	0.01	0.01	15.31
Sandy land	2.72	6.17	0.61	0	0.09	0.16	0.02	9.77
Woodland	0.07	2.48	14.42	1.22	0.29	0.08	0.09	18.65
Garden	0	0	0.32	0.56	0.03	0	0	0.91
Farmland	0.11	0.45	4.43	1.18	6.41	0.16	0.35	13.09
River	0.04	0.18	0.22	0.02	0.25	0.29	0.17	1.17
Residential land	0.18	0.22	0.15	0	0.21	0	0.88	1.64
Total	18.32	9.56	20.15	2.98	7.31	0.70	1.52	60.54

Table 7. *Transition matrix of different land use types along the eastern coast of Laizhou Bay from* 1985 *to* 1998(km^2)

1985–1998	Sea	Sandy land	Woodland	Farmland	River	Residential land	Aquaculture land	Total
Sea	17.69	0.37	0	0	0	0.14	0	18.20
Sandy land	1.57	3.39	0.27	0.42	0.12	0.46	3.29	9.52
Woodland	0.02	1.74	14.13	0.83	0.22	0.14	3.02	20.10
Garden	0	0	1.45	1.42	0	0.01	0.10	2.98
Farmland	0.03	0.12	0.84	4.82	0.11	0.85	0.48	7.25
River	0.11	0.06	0.02	0.03	0.38	0.01	0.04	0.65
Residential land	0.02	0.03	0	0.03	0	1.43	0	1.51
Total	19.44	5.71	16.71	7.55	0.83	3.04	6.93	60.21

Table 8. *Transition matrix of different land use types along the eastern coast of Laizhou Bay from* 1998 *to* 2006(km^2)

1998–2006	Sea	Sandy land	Woodland	Farmland	River	Residential land	Aquaculture land	Total
Sea	17.54	0.52	0	0.01	0.01	1.03	0.32	19.43
Sandy land	0.08	1.30	0.58	0.43	0.17	0.25	2.97	5.78
Woodland	0	0.02	12.50	3.32	0.07	0.44	0.38	16.73
Farmland	0	0.01	2.56	3.55	0	1.14	0.28	7.54
River	0.17	0.02	0.22	0.14	0.43	0.01	0.10	1.09
Residential land	0.01	0	0.14	0.03	0	2.71	0.14	3.03
Aquaculture land	0	0.23	1.08	0.22	0.06	0.11	5.26	6.96
Total	17.80	2.10	17.08	7.70	0.74	5.69	9.45	60.56

Table 9. *Transition matrix of different land use types along the eastern coast of Laizhou Bay from* 2006 *to* 2013(km^2)

2006–2013	Sea	Sandy land	Woodland	Farmland	River	Residential land	Aquaculture land	Total
Sea	16.50	0.30	0	0	0.02	0.78	0.07	17.67
Sandy land	0.21	1.02	0.19	0	0.03	0.06	0.50	2.01
Woodland	0	0.04	10.71	4.30	0.15	0.53	1.39	17.12
Farmland	0	0.06	2.74	3.26	0.09	0.68	0.83	7.66
River	0.03	0.02	0.05	0.02	0.45	0	0.18	0.75
Residential land	0.08	0.02	0.28	0.03	0	4.91	0.40	5.72
Aquaculture land	0.11	0.34	0.08	0.10	0.03	0.41	8.39	9.46
Total	16.93	1.80	14.05	7.71	0.77	7.37	11.76	60.39

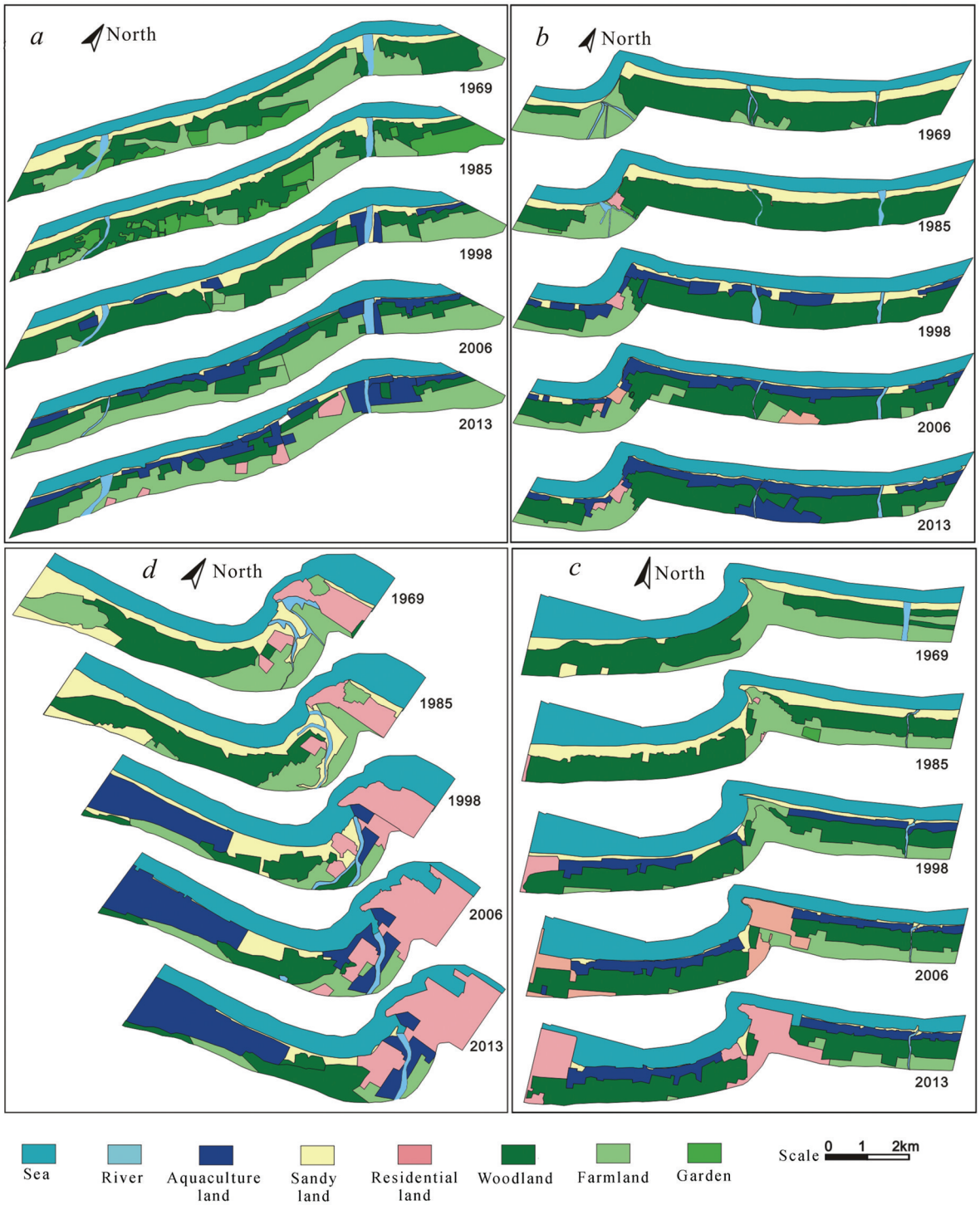

Figure 4. Spatial distribution changes of land use along the eastern coast of Laizhou Bay during the recent 50 years

In order to reveal the spatial distribution pattern of land use and its change along the coastal zone, the eastern coast of Laizhou Bay (Jiehekou-Diaolongzui spit) is divided into four sub-coasts of a, b, c, d, whose land use change is drawn in Figure 4. Figure 4 shows that the land use exhibit pattern of strips parallel to the coastline in the sequence of sea, sandy land, woodland and farmland in 1969. In 1985, garden presenting uncontinuous block distribution between woodland and farmland (Figure 4). Since 1998, most of the sandy land in the supratidal zone has been converted into aquaculture ponds of large area, and the distribution pattern of the aquaculture ponds gradually evolved from the uncontinuous block to the continuous strip between sea and woodland (Figure 4).

Morphodynamic effects of the narrowing supratidal zone

In this section, we present the numerical results of wave height, current velocity and geomorphic evolution along the above three different profiles (Figure 2), which are extracted from the area series results computed by the Mike model.

From the numerical simulation results we can see that wave heights under the condition of land use rate reaching 30% and 70% are higher than that of under the condition of unused supratidal zone along the three profiles 1-1, 2-2 and 3-3 (Figure 5). The increase of wave height is not monotonous with the increase of land use because the wave reflection is different for the different vertical wall boundary in the Mike model. All of the wave heights along the three profiles reduce fluctuantly from sea to land but their fluctuant characteristics are very different due to the different bottom friction (Figure 5). The wave change features for the same profile are different under the condition of the different land use rate because the factory aquaculture facilities modify the boundary conditions of coastal ocean dynamics.

Land use along the supratidal zone significantly enhance the nearshore current velocities and this effects are nonlinear. The current velocities along the different profiles increase with the increase of the land use rate and present the trend of decrease firstly-increase then-decrease finally from sea to land. The highest current velocities along the profiles 1-1, 2-2 and 3-3 appears near the coastline and are about 0.36 m/s, 0.41 m/s and 0.40 m/s, respectively (Figure 6).

The profiles 1-1, 2-2 and 3-3 are located in the lower, middle and upper coasts of the study region, respectively (Figure 2). Impacted by the storm surge for 12 hours, under the different land use rate, the profiles 1-1 and 2-2 keeps dynamic equilibrium except for the regions near the coastline. The erosion along the profile 3-3 becomes more serious than that along the profiles 1-1 and 2-2 and expand to the scope of 5.0 km away from the coastline. Impacted by the storm surge for 24 hours, under the different land use rate, the erosion along the three profiles becomes more obvious than that impacted by the storm surge for 12 hours. The erosion along the profiles 1-1 and 2-2 is quite obvious near the coastline and occurs slightly within the scope of 6 km away from the coastline. The erosion of the profile 3-3 is significantly serious within the scope of 5.0 km away from the coastline (Figure 7). Coastal erosion in the study region becomes more serious with the increase of the land use rate and the increase extent is very different for the different profiles.

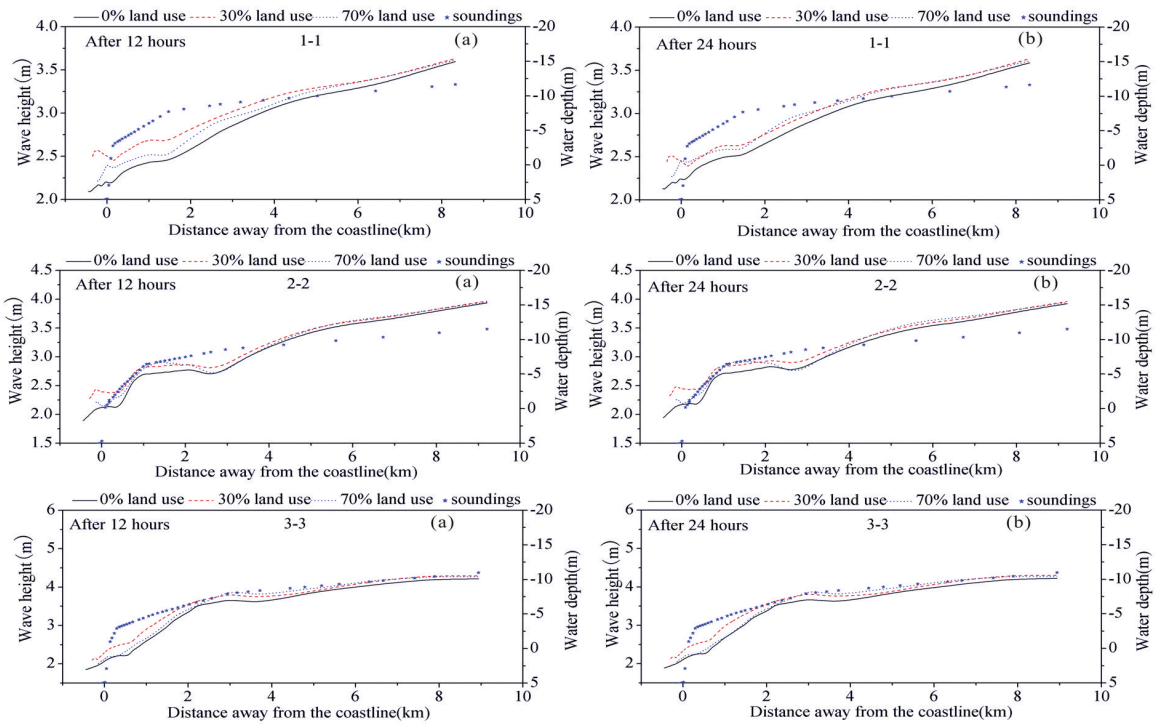

Figure 5. Wave height and water depth along the profiles 1-1, 2-2 and 3-3 under the different conditions ((a) for 12 hours and (b) for 24 hours)

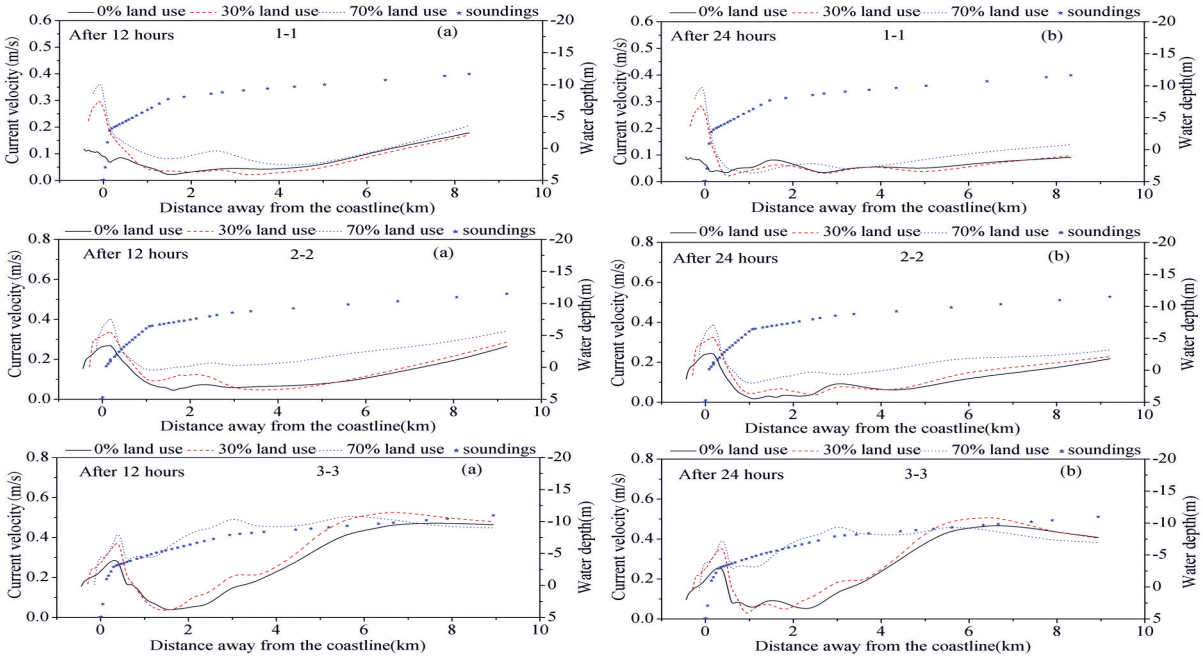

Figure 6. Current velocity and water depth along the profiles 1-1, 2-2 and 3-3 under the different conditions((a) for 12 hours and (b) for 24 hours)

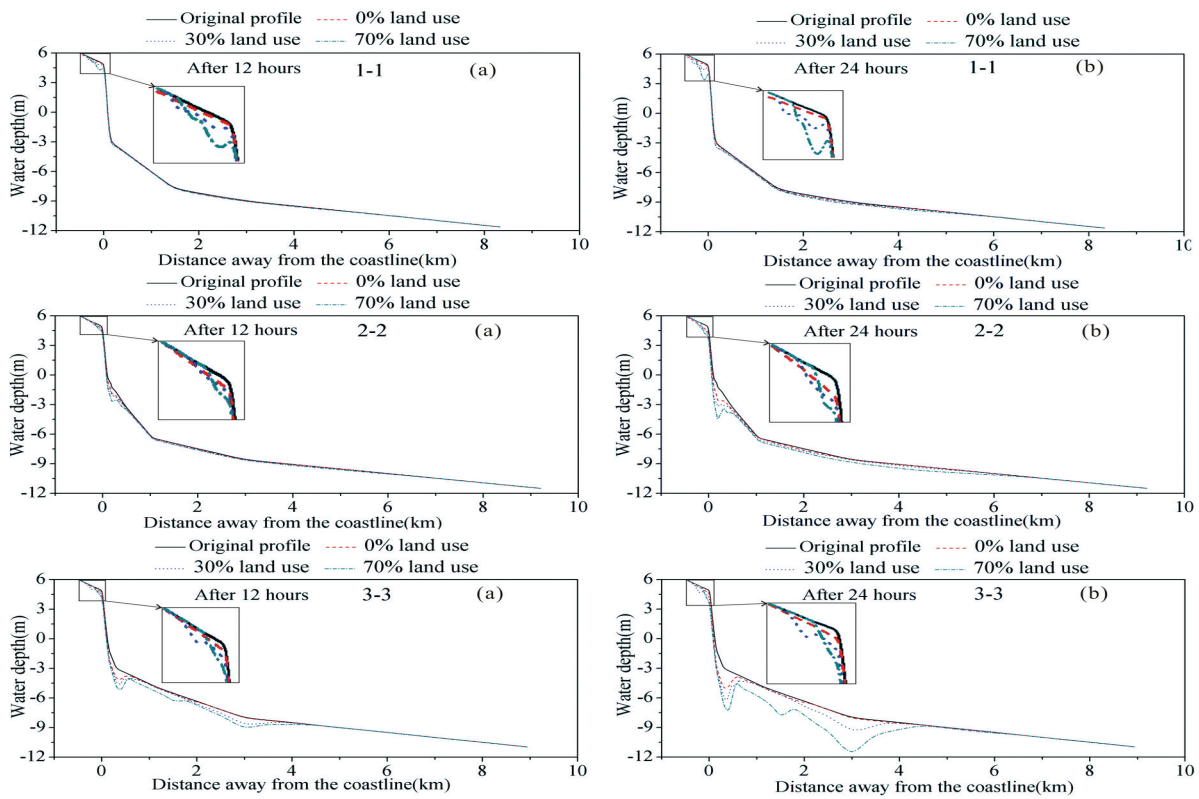

Figure 7. The geomorphic evolution of the profiles 1-1, 2-2 and 3-3 under the different conditions((a) for 12 hours and (b) for 24 hours)

DISCUSSION

Driving force of land use change

Before the middle 1980s, apart from some small fishing piers, simple roads, and isolated houses built in some regions, the supratidal zone located in the eastern coast of Laizhou Bay was dominated by the coastal sandy land. Coastal erosion was mainly a result of reduced fluvial sediment transport resulted from the construction of the reservoirs located in the middle and upper reaches of the rivers since the 1960s. The spatial succession of land use/land cover was farmland, shelter forest, sandy land, and sea. Besides, the boundaries between the adjacent different land use types moved landward as a result of coastal erosion.

During the 30 years after the middle 1980s, the supratidal sandy land was gradually developed and used in the form of shrimp farming, scallop farming, turbot farming and trepang farming along the eastern coast of Laizhou Bay (Figure 3). Among them, shrimp farming fishery was started in 1978 along the supratidal zone, which showed the characteristics of slow development, small farming scale and low yield at an early stage. As the factory artificial breeding of shrimp farming achieved a major breakthrough and spread in China in 1982, shrimp farming fishery has entered into the phase of rapid development along the eastern coast of Laizhou Bay since 1985. The shrimp farming area of Laizhou city was only 3290 hm^2 (yield of 1703t) in 1985, while in 1989 the area exceeded $2\times10^5 hm^2$ (yield of 18776t).

Scallop farming emerged rapidly as a new fishery along the eastern coast of Laizhou Bay in 1993. The turbot farming developed rapidly along the eastern coast of Laizhou Bay in 1999. In 2006, more than 1300 supratidal factory farming greenhouses existed along the coast of Laizhou with total area of farming exceeded 700 000 m^2. After many iterative rounds of development – expansion – shrink and structural adjustment for more than 30 years, the aquaculture fishery of the eastern Laizhou Bay has entered the phase of factory aquaculture, whose technical level and spatial agglomeration scale are highest in the Chinese sandy coast.

Morphodynamic effects of the narrowing supratidal zone

Our field surveys show that most of the supratidal sandy land along the eastern coast of Laizhou Bay has been converted to aquaculture ponds or greenhouses in the last 30 years. At the same time, the extent and scale of coastal erosion continued to broaden and erosive scarps has been found everywhere as a belt zone of aquaculture facility was formed (Figure 3). Thus it can be seen that the construction of aquaculture facility caused serious coastal erosion. And this fact is consistent with the numerical results.

According to the hydrodynamic numerical results of the different land use, coastal erosion is more obvious and serious with the increase of the land use extent. The research results may have important practical implications for the reasonable construction of aquaculture facility along the eastern coast of Laizhou Bay. Furthermore, this coast belongs to a typical sandy coast affected the temperate monsoon climate. The coastal erosion, the construction of reservoirs and the development speed of aquaculture facilities are representative among the Chinese mountainous coasts in the recent 50 years. So the research results will deepen the understanding of the causes of the coastal erosion under the background of global changes.

The large-scale construction of the factory aquaculture facilities in the last 30 years, that causes the supratidal zone to become narrower and narrower or even disappear along the eastern coast of Laizhou Bay. As a result, the oceanic dynamic effects near the coast are significantly enhanced to give rise to the erosion of coastline, beach and underwater coastal sea slope. This may be one of the main reasons for the continuously expanded erosion along the eastern coast of Laizhou Bay in the recent 30 years.

CONCLUSIONS

Land use change along the eastern coast of Laizhou bay has been very significant in the recent 50 years. The areas of sea and woodland first increased and then decreased. The areas of residential land and aquaculture land began to increase rapidly after 1985, while the areas of sandy land and farmland decreased. During the last 50 years especially the last 30 years, there has been a main evolution trend of shifting from aeolian sandy land, woodland and farmland to aquaculture ponds and residential land. A continuous belt zone of aquaculture facility has been formed to change profoundly the hydrodynamic boundary conditions of storm surges. The ocean dynamic was significantly enhanced and caused severe erosion of the beach and underwater coastal sea slope near the coastline. The erosion along the eastern coast of Laizhou Bay became more obvious with the increase of supratidal land use rate.

ACKNOWLEDGEMENTS

This research was jointly supported by the National Natural Science Foundation of China (NSFC, Grants Nos. 41071011, 41271016 and 41471005), a Project of Shandong Province Higher Educational Science and Technology Program (Grant No. J14LH02) and Yantai Science and Technology Development Program Project (Grant No. 2014ZH075). The authors express sincere thanks to National Natural Science Foundation of China and anonymous reviewers.

LITERATURE CITED

Airoldi, L. and Beck, M. W., 2007. Loss status and trends for coastal marine habitats of Europe. *Oceanography and Marine Biology: An Annual Review*, 45, 345–405.

Bird, E. C. F., 1996. *Beach Management*. New York: John Wiley, 281p.

Chang, R. F.; Zhuang, Z. Y., and Wu, J. M., 1993. Retrogression and protection of the north – west coast of the Shandong Peninsula. *Journal of Ocean University of Qingdao*, 23(3), 60–68 (in Chinese).

Defeo, O.; Mclachlan, A.; Schoeman, D. S.; Schlacher, T. A.; Dugan, J.; Jones, A.; Lastra, M., and Scapini, F., 2009. Threats to sandy beach ecosystems: a review. *Estuarine, Coastal and Shelf Science*, 81(1), 1–12.

Durgappa, R., 2008. Coastal Protection Works. *Proceedings7th International Conference of Coastal and Port Engineering in Developing Countries, COPEDEC VII* (Dubai), Paper 97, PP. 1–15.

Edition Committee of the Bay Chorography in China, 1993. *The Bay Chorography in China* (3). Beijing: Ocean Press, 487p (in Chinese).

Komar, P. D. and Allan, J. C., 2008. Increasing hurricane-

generated wave heights along the U. S. east coast and their climate controls. *Journal of Coastal Research*, 24(2), 479-488.

Splinter, K. D.; Davidson, M. A.; Golshani, G., and Tomlinson, R., 2012. Climate controls on longshore sediment transport. *Continental Shelf Research*, 48(1), 146-156.

Short, A. D. and Masselink, G., 1999. Embayed and Structurally Controlled Beaches. *Handbook of Beach and Shoreface Morphodynamics*. (Wiley, New York), pp. 230-249.

Wang, Q.; Yang, H.; Zhong, S. Y.; Du, G. Y.; Zhang, Y. J., and Gao, G. C., 2003. Sedimentary dynamics and geomorphic evolution of the Laizhou shoal. *Acta Geographica Sinica*, 58(5),749-756(in Chinese).

Mather, A. A., 2008. Sea level rise for the east coast of Southern Africa. *Proceedings 7th International Conference of Coastal and Port Engineering in Developing Countries*, *COPEDEC VII* (Dubai, UAE), Paper M-04, pp. 1-11.

Xia, D. X., 2009. *Geomorphic environment and its evolution in the coastal zones*. Beijing: Ocean Press,314p(in Chinese).

Zhang, K. Q.; Douglas, B. C., and Leatherman, S. P., 2004. Global warming and coastal erosion. *Climate Change*, 64, 41-58.

Zhuang, Z. Y.; Chen, W. M., and Xu, W. D., 1989. Retrogression of straight sandy beaches in the Shandong Peninsula and its results. *Journal of Ocean University of Qingdao*, 19(1),90-98(in Chinese).